



# Vapour Transport in Low Permeability Unsaturated Soils with Capillary Effects

S. OLIVELLA and A. GENS

*Geotechnical Engineering and Geosciences Department Universidad Politecnica de Catalunya  
Barcelona, Spain*

(Received: 22 January 1999; in final form: 11 January 2000)

**Abstract.** A discussion of water phase change in unsaturated soils that develop capillary effects is first carried out in the paper. A distinction between the GR (geothermal reservoir) and the NUS (nonisothermal unsaturated soil) approaches is performed. Several aspects concerning advective and nonadvective fluxes of vapour are described secondly and some relationships concerning the case of mass motion in a closed system subjected to temperature gradients derived. Since the structure of unsaturated clays changes with moisture content, in order to correctly simulate the coupled phenomena induced by temperature gradients a model for intrinsic permeability as a function of humidity is required. A preliminary version of the model is presented and applied to interpret a laboratory test by means of a numerical simulation using CODE\_BRIGHT.

## 1. Introduction

The main purpose of this paper is to review some aspects related to water phase change into vapour form and its transport in the context of unsaturated soil behaviour. Also a model for intrinsic permeability that can explain some features observed in clays is presented. A number of problems require a good knowledge of the vapour phase change and migration in unsaturated soils. This problem of water phase change and vapour transport in porous media has been treated in different ways depending on the area of interest.

In the context of radioactive waste disposal low permeability soils are used for building isolating barriers. These clays are initially unsaturated, have swelling properties and are subjected to wetting – drying/heating cooling cycles. Depending on the possibility of structure change induced by chemical effects, temperature may be limited (typically 100°C). At 100°C the vapour pressure is 0.1 MPa according to the phase diagram of pure water. Although surface tension effects reduce vapour pressure in equilibrium, the total gas pressure ( $P_g = P_a + P_v$ , i.e. gas pressure equals air pressure plus vapour pressure) can not, in general, be considered constant.

Philip and De Vries (1957) early investigated thermal effects in unsaturated soils. Later, Milly (1982) extended their work to heterogeneous and hysteretic medium. The theoretical approach followed by these soil scientists assumes that air

flow can be neglected which is an adequate assumption in a number of situations. The soil scientists' approach is based on matric head and temperature as state variables. As mentioned below, calculation of  $P_g = P_v + P_a$  is required for checking desaturation caused by heating. In hydro-thermal calculations near the soil surface, atmospheric pressure is a sufficient reference to define soil desaturation, but this is not an adequate assumption in problems related to radioactive waste disposal.

These formulations were later extended to include the presence of air. For instance, Pollock (1986) presents a multiphase approach incorporating the balance of air. In that work liquid saturation, gas pressure and temperature are used as state variables. Of course, liquid saturation is not an adequate choice for saturated zones of the porous medium but it can be easily changed by liquid pressure. If saturation occurs, one only needs to check the condition of  $P_g > P_l$  in order to know if the soil is unsaturated. Since gas pressure is composed by vapour pressure plus air pressure ( $P_g = P_v + P_a$ ), a temperature increase induces vapour pressure increase and this may induce a desaturation of an initially saturated soil.

Another area of research related to thermal effects in geological media is the field of geothermal energy. A reference work by Faust and Mercer (1979) contains the basic formulation for modelling geothermal reservoirs. Although there are points in common with the work of the above-mentioned soil scientists, the approaches used in these two investigation fields are conceptually different. Following the geothermal reservoir approach, it is possible to handle the problem of phase change induced by heating. However, in this approach capillary effects and the possible presence of air are neglected.

More recently, interest in this topic has increased also due to the environmental problems related to organic compounds. A relevant work has been presented by Falta *et al.* (1992) with the objective of modelling the process of steam injection for the removal of NAPL (nonaqueous phase liquids) in contaminated soils. One aspect that makes this approach more complex than the preceding ones is the flow in three phases and with three components (water, air and NAPL).

Bear and Gilman (1995) have investigated the migration of salts in the unsaturated zone induced by heating. A related work is presented in Olivella *et al.* (1996a) where porosity variations in saline media caused by temperature gradients were investigated. In both works, it is shown that the liquid flux induced by vapour migration is able to transport dissolved salts from the cold toward the hot side. Characterization of water flow induced by vapour migration may be of substantial interest for modelling solute transport processes in soils.

In this paper, the theoretical aspects of phase change are presented first with special attention to the case of phase change under unequal phase pressures. It is discussed why the geothermal reservoir approach is not applicable to unsaturated soil behaviour. On the other hand, it will be shown that the approach that takes into account capillary effects and presence of air is more general and reduces to the geothermal reservoir approach when applied to a soil that develops small suctions.

In the third section, the theory for vapour flow in unsaturated soils is reviewed with special attention to the reasons for flux enhancement due to air immobility and the pressure gradients induced by temperature gradients. The widely used approximation in which the equation of air balance is not solved may cause vapour flux enhancement.

Liquid and gas permeability is the subject of the fourth section. It has been observed that for clays, even at constant porosity, it is not possible to consider that the intrinsic permeability remains constant with respect to water content. In fact, the structure of the soil changes with water content. A model to take into account this effect is proposed. By means a very simple double structure approach it is possible to model the variation of intrinsic permeability with degree of saturation. The model may simulate flow in clays that show a maximum permeability before full saturation is achieved.

Finally, an example of application of this model will be presented in which water flow induced by temperature gradients takes place. The example is calculated using CODE\_BRIGHT (Olivella *et al.*, 1996b), which is a finite element code for solving coupled thermo-hydro-mechanical problems (mechanical effects are beyond scope of this paper). The application that is presented is related to problems of radioactive waste disposal in underground openings including barriers of low permeability porous materials. It is shown that the proposed model allows a more suitable modelling of the drying process induced by temperature gradients than the usually adopted one that considers intrinsic permeability only a function of porosity.

## 2. Phase Change of Water: Importance of Capillary Effects

### 2.1. PHASE CHANGE OF WATER WITHOUT CAPILLARY EFFECTS: THE GR APPROACH

The Phase change diagram for pure water is represented in Figure 1 (see for instance Faust and Mercer, 1979) which displays that there are several regions. Depending on the pressure of water ( $p$ , MPa) and the enthalpy per unit mass of water ( $h$ , J/kg) three regions are distinguished: liquid-phase region, two-phase region and gas-phase region.

The phase diagram displayed in Figure 1 represents also the behaviour of water in a soil if it can be assumed that capillary forces are negligible, in other words, surface tension is assumed zero. This implies that water and vapour pressures are equal, and then capillary pressure is equal to zero.

The geothermal reservoir (GR) approach (Faust and Mercer, 1979) uses this diagram and, among other laws, the equations representing it are introduced in the mass and energy balance equations. For water, density and enthalpy are defined as

$$\rho = \rho_l S_1 + \rho_v (1 - S_1) \quad (1)$$

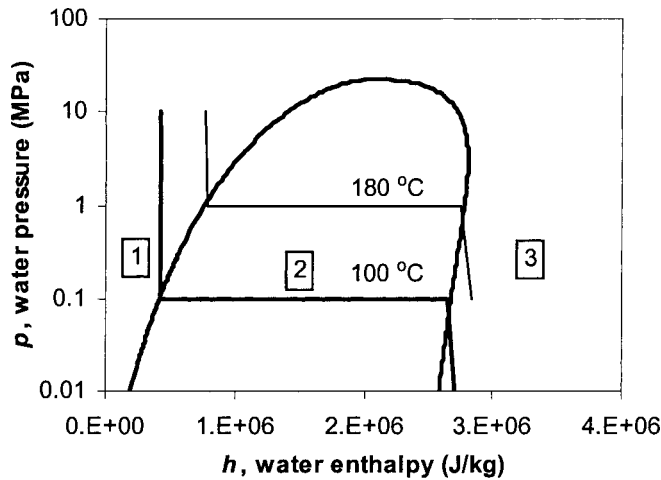


Figure 1. Pressure-enthalpy diagram for pure water. Two isotherm lines (100°C and 180°C) are represented; 1, Single phase region (liquid water); 2, Two phase region (liquid water + vapor); 3, Single phase region (heated vapor).

and

$$h = \frac{h_l \rho_l S_l + h_v \rho_v (1 - S_l)}{\rho}, \quad (2)$$

where  $S_l$  is degree of saturation, that is, volume of liquid per unit volume of voids;  $\rho_v$  is density of water vapour;  $\rho_l$  is density of liquid water;  $h_v$  is enthalpy of water vapour, and  $h_l$  is enthalpy of liquid water.

Following the geothermal reservoir approach, the state variables that are usually selected are the pressure ( $p$ ) and the enthalpy ( $h$ ). From these variables the others are calculated. Several empirical functions allow to calculate density, enthalpy of liquid water and vapour and temperature (see for instance Roberts *et al.*, 1987). Degree of saturation is obtained from (2). In the formulation for GR it is assumed that air is not present in the soil. Therefore, voids are filled with liquid water plus pure water vapour (region 2) or only one of them (regions 1 and 3). As vapour progressively condenses the soil progressively saturates and vices versa.

Following this diagram, the variation of temperature and degree of saturation as a function of enthalpy for a saturated soil with negligible capillary forces (e.g. coarse granular soil) that is heated at two pressures (0.1 MPa and 1 MPa) have been calculated (Figures 2 and 3). Since pressure is constant, this heating process is represented in Figure 1 by a horizontal line that crosses the three regions from the left to the right. Figure 2 shows that temperature is constant during the evaporation of water, that is, when the pressure/enthalpy point falls in region 2. Figure 3 shows the process of desaturation that begins at 100°C and finishes when degree of saturation tends to zero. As soon as all water is evaporated temperature starts again to increase.

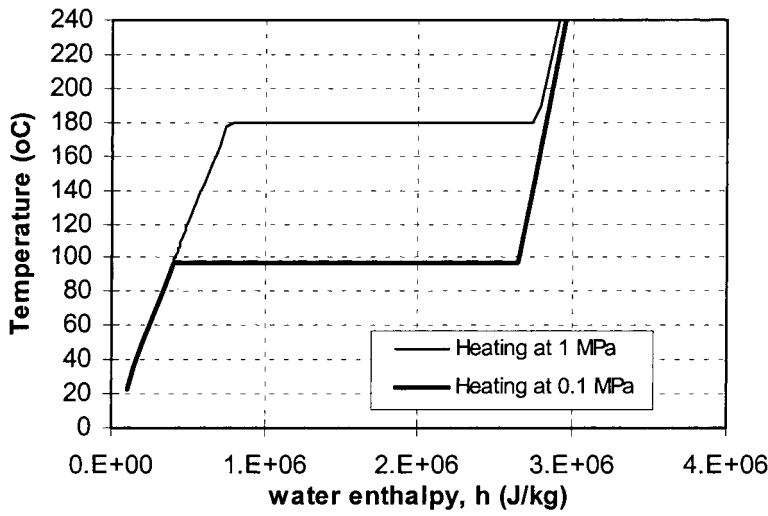


Figure 2. Temperature vs water enthalpy for heating a granular soil at 0.1 MPa (atmospheric pressure) and at 1 MPa.

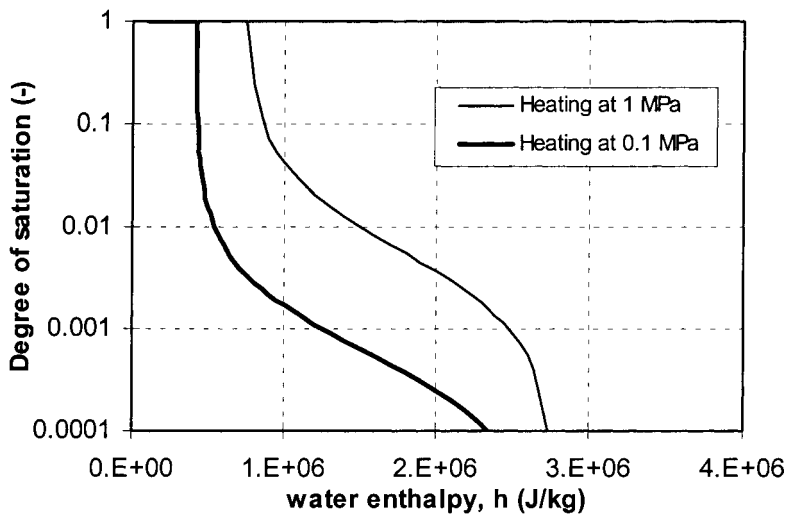


Figure 3. Degree of saturation vs enthalpy for heating a granular soil at 0.1 MPa (atmospheric pressure) and at 1 MPa.

It should be pointed out that the assumption of negligible capillary forces implies that for a given pressure and enthalpy, degree of saturation is unambiguously determined using only the phase change diagram. As explained below, this is clearly in contrast to what happens in a soil where capillary effects are not negligible.

## 2.2. PHASE CHANGE OF WATER WITH CAPILLARY EFFECTS: THE NUS APPROACH

When capillary effects can not be neglected water phase change in a soil incorporates different features. Liquid water and water vapour have different pressures. The implications are the following:

- Degree of saturation can be obtained from a retention curve that relates capillary pressure (gas pressure minus liquid pressure). The shape of the curve can, however, change with temperature. In fact, a model for retention curve should incorporate a dependence on surface tension so the temperature influence on the meniscus radius is properly accounted (Milly, 1982).
- Vapour density is modified by capillary pressure according to psychometric law (Edlefsen and Anderson, 1943). The drier the soil, the lower the relative humidity with respect to the case in planar surface state.
- Surface tension is a decreasing function of temperature. Therefore at high temperatures the behaviour of phase change should tend towards the situation without capillary effects.

The nonisothermal unsaturated soil (NUS) approach is used for modelling the nonisothermal multiphase flow of water and gas through a soil. This approach takes into account capillary effects and also it considers the possible presence of air in the soil. Philip and De Vries (1957) first established this approach. With this background, several approaches have been developed and used for modelling unsaturated soil behaviour (among others: Milly, 1982; Olivella *et al.*, 1994). The formulation developed by Olivella *et al.* (1994) has been used to build CODE\_BRIGHT (Olivella *et al.*, 1996b) which is a finite element code that solves coupled thermo-hydro-mechanical problems. The formulation implemented in this code contains also features such as mechanical effects and dissolution/precipitation of salt. In fact, it was first established for saline media.

In order to see the influence of capillary effects on phase change a sensitivity analysis (Appendix 1) using CODE\_BRIGHT (in Appendix 2 the balance equations that are solved are included), which is essentially based on the NUS approach, has been performed. The retention curve of van Genuchten (1980) has been chosen because it is widely used to represent unsaturated soil behaviour. This law can be written as

$$S_e = \frac{S_l - S_{\min}}{S_{\max} - S_{\min}} = \left[ 1 + \left( \frac{P_g - P_l}{P} \right)^{1/(1-\lambda)} \right]^{-\lambda} \quad (3)$$

This equation contains the parameters  $\lambda$  and  $P$ . The first ( $\lambda$ ) essentially controls the shape of the curve while the second ( $P$ ) controls its height, so this latter can be interpreted as a measure of the capillary pressure required to start the desaturation

of the soil. Since capillary pressure can be scaled with surface tension (Milly, 1982) it appears that  $P$  also does. This can be shown if Laplace's law is recalled

$$P_g - P_l = \frac{2\sigma}{r}, \quad (4)$$

where  $\sigma$  is surface tension and  $r$  is the curvature radius of the meniscus and Equation (3) is rewritten as

$$P_g - P_l = P(S_e^{-1/\lambda} - 1)^{(1-\lambda)} \quad (5)$$

then, if it is assumed that constant water content implies both  $S_e$  constant and  $r$  constant, it follows that

$$P = P_o \frac{\sigma(T)}{\sigma(T_o)}, \quad (6)$$

where  $P_o$  is the corresponding parameter at temperature  $T_o$ . This means that  $P$  will decrease with temperature because surface tension also does. Consequently suction will decrease with temperature for a given degree of saturation.

Finally, it must be said that the presence of air is naturally handled in the NUS approach. In fact, in most of cases soils are unsaturated due to the presence of air but not due to water phase change. On the contrary, the GR approach cannot handle the presence of air as it is usually used by geothermal reservoir modellers. If it is assumed that vapour and air behave as perfect gases, the gas phase pressure is  $P_g = P_a + P_v$ . In absence of capillary effects, the gas phase pressure should be equal to the liquid phase pressure. Then, the vapour pressure cannot be equal to the liquid water pressure as assumed in the phase diagram. Or, from another point of view, if vapour pressure is equal to liquid pressure then gas pressure is higher than liquid pressure and this implies surface tension effects.

### 3. Vapour Flow in an Unsaturated Soil

In Wa'il Abu-El-Sha'r and Abriola (1997) the existing approaches for modelling gas flow in porous media are reviewed. According to these authors the DGM (dusty gas model) approach should be used for modelling flow of gas mixtures in porous media. Since this approach is not yet widely used, as agreed by these authors, we will still apply the usual formulation based on First Fick's law.

#### 3.1. MECHANISMS OF VAPOUR FLOW

The mechanisms of vapour flow in an unsaturated soil can be classified as advection, diffusion and dispersion. These fluxes can be expressed below.

First, advective flux is calculated as

$$(\mathbf{i}_g^w)_{\text{advection}} = \rho_g^w \mathbf{q}_g = \omega_g^w \rho_g \mathbf{q}_g, \quad \mathbf{q}_g = \frac{-k_{rg} \mathbf{k}}{\mu_g} (\nabla P_g + \rho_g \mathbf{g} \nabla z), \quad (7)$$

where  $\omega_g^w$  is mass fraction of water in gas,  $\rho_g$  is gas density,  $\mathbf{k}$  is the intrinsic permeability tensor,  $k_{rg}$  is gas relative permeability,  $\mu_g$  is gas viscosity,  $g$  is gravity and  $P_g$  is gas pressure. Equation (17) is generally considered valid either for a gas phase composed by pure vapor ( $\omega_g^w = 1$ ) or either by a mixture of air and vapour ( $\omega_g^w < 1$ ). Generalised Darcy's law (Bear, 1972) is usually used to calculate the volumetric phase flux. Of course, the viscosity of the phase can be considered a function of its composition and temperature.

The above-described advective flux has been written under the assumption of laminar flow. When the pores are small and the pressure is also low, the mean free path of gas molecules may be comparable to the pore sizes. When this happens, slip takes place and the assumption of purely laminar flow is no longer valid. A simple modification of Equation (7) to account for Knudsen diffusion consists in using an apparent intrinsic permeability with the following form (Wa'il Abu-El-Sha'r and Abriola, 1997):

$$\mathbf{k}_a = \mathbf{k} + \mathbf{I} \frac{D_k \mu_g}{P_g}, \quad (8)$$

where  $D_k$  is the Knudsen diffusion coefficient and  $\mathbf{I}$  is the identity matrix.

Second, diffusive flux is calculated as

$$(\mathbf{i}_g^w)_{\text{diffusion}} = -(\mathbf{D}_g^w)_{\text{diffusion}} \nabla \omega_g^w, \quad (\mathbf{D}_g^w)_{\text{diffusion}} = \tau \phi D \mathbf{I} S_g \rho_g, \quad (9)$$

where  $\tau$  is tortuosity,  $\phi$  is porosity,  $D$  is a molecular diffusion coefficient for vapour in air and  $S_g$  is degree of saturation of gas phase. Equation (9) has been written as a generalised form of Fick's law for molecular diffusion in porous media.

And third, dispersive flux is calculated as

$$\begin{aligned} (\mathbf{i}_g^w)_{\text{dispersion}} &= -(\mathbf{D}_g^w)_{\text{dispersion}} \nabla \omega_g^w, \\ (\mathbf{D}_g^w)_{\text{dispersion}} &= \rho_g \left[ d_l |\mathbf{q}_g| \mathbf{I} + (d_l - d_t) \frac{\mathbf{q}_g - \mathbf{q}_g^t}{|\mathbf{q}_g|} \right], \end{aligned} \quad (10)$$

where  $d_l$  and  $d_t$  are dispersivities. In Equation (10) Fick's law is used but with the corresponding tensor to model dispersion of a component in a phase that is flowing in a porous medium (Bear, 1972). Both diffusion and dispersion vanish, as the gas phase becomes a single component phase. This is well represented by Equations (9) and (10) because mass fraction ( $\omega_g^w$ ) becomes constant and equal to 1 and, consequently, the gradient of mass fraction becomes zero.

Coupled processes (e.g. advective flux due to temperature or concentration gradients; non advective fluxes due to pressure gradients) are not considered here.

Finally the total flux of vapour can be written as

$$\mathbf{j}_g^w = (\mathbf{i}_g^w)_{\text{advection}} + (\mathbf{i}_g^w)_{\text{diffusion}} + (\mathbf{i}_g^w)_{\text{dispersion}} = \omega_g^w \rho_g \mathbf{q}_g - \mathbf{D}_g^w \nabla \omega_g^w, \quad (11)$$

where, as usual, the diffusive and the dispersive terms have been put together. And a similar expression holds for air flux

$$\mathbf{j}_g^a = (\mathbf{i}_g^a)_{\text{advection}} + (\mathbf{i}_g^a)_{\text{diffusion}} + (\mathbf{i}_g^a)_{\text{dispersion}} = \omega_g^a \rho_g \mathbf{q}_g - \mathbf{D}_g^a \nabla \omega_g^a. \quad (12)$$



The gas phase is considered a binary mixture of two species (vapour and air) in which an influence of each species motion is exerted on the other species motion. According to Bird *et al.* (1960) in a binary system the mass fluxes of species with respect to the mass averaged velocity of the phase are zero. If it can be assumed that the mass averaged velocity coincides here with  $\mathbf{q}_g$  then it should follow that  $\mathbf{D}_g^w = \mathbf{D}_g^a$ . On the contrary, if Darcy's flux ( $\mathbf{q}_g$ ) gives the volume (or molar) averaged velocity (Bear and Bachmat, 1986) then mass fractions can be substituted by molar fractions and the same result is obtained (i.e.  $\mathbf{D}_g^w = \mathbf{D}_g^a$ ). In this latter case, if mass fractions are still used in calculating (9) and (10) then it is required to use  $\mathbf{D}_g^w \neq \mathbf{D}_g^a$ . The ratio between these two coefficients is equal to the ratio between the molar mass of air (28 g) and the molar mass of vapour (18 g) approximately 1.5. Bear and Gilman (1995) still use  $\mathbf{D}_g^w = \mathbf{D}_g^a$  in a mass fraction based formulation, so here it is also considered to hold.

### 3.2. LOW VAPOUR CONCENTRATION VERSUS HIGH VAPOUR CONCENTRATION

If the fluxes in Equation (12) are split then

$$\begin{aligned} \mathbf{j}_g^w &= \omega_g^w \rho_g \mathbf{q}_g - \mathbf{D}_g^w \nabla \omega_g^w \\ &= -\omega_g^w \rho_g \frac{k_{rl} \mathbf{k}}{\mu_g} \nabla P_g - \left( d_l |\mathbf{q}_g| \mathbf{I} + (d_l - d_t) \frac{\mathbf{q}_g \mathbf{q}_g^t}{|\mathbf{q}_g|} \right) \rho_g \nabla \omega_g^w - \\ &\quad - (\tau \phi S_g D \mathbf{I}) \rho_g \nabla \omega_g^w, \end{aligned} \quad (13)$$

where, without loss of generality, the gravity term in the Darcy's law has been neglected assuming that the flow is horizontal. In this equation,

- The third term is dominant in low vapour concentration situations if there are no external pressure gradients. This is the case of an unsaturated soil subjected to a moderate temperature and temperature gradient.
- The first one is dominant when the gas phase is pure vapour. In this case, the second and the third vanish because  $\omega_g^w = 1$ . For the case of low vapour concentrations, the first term may become important if an external pressure gradient is imposed.
- The second term is only important if both mass fraction and pressure gradients are considered. However, the high molecular diffusivity of vapour in air usually leads to neglect this dispersion term.

Equation (13) contains four material parameters that control the process of vapour transport. The two dispersivities ( $d_l$  and  $d_t$ ) enter in the second term and since vapour molecular diffusion is very efficient, specially if temperature is high, dispersion will be neglected. The other two material parameters are intrinsic permeability ( $\mathbf{k}$ ) and tortuosity ( $\tau$ ).

### 3.3. FLUX ENHANCEMENT DUE TO AIR IMMOBILITY

When a nonisothermal flow problem is simulated, simplifications can be performed in order to avoid solving the air mass conservation equation. The following two possibilities considered here are (a) air immobility and (b) constant gas pressure. In any case, dissolved air is neglected, that is, air is only present in the gas phase.

(a) Bear and Gilman (1995) have shown that the assumption of air immobility implies an enhancement of vapour diffusion. This is explained in the following way considering that the total air flux is zero

$$\mathbf{j}_g^a = \omega_g^a \rho_g \mathbf{q}_g - \mathbf{D}_g^a \nabla \omega_g^a = 0, \quad \rho_g \mathbf{q}_g = \frac{1}{\omega_g^a} \mathbf{D}_g^a \nabla \omega_g^a = \frac{-1}{1 - \omega_g^w} \mathbf{D}_g^w \nabla \omega_g^w. \quad (14)$$

Which can be introduced in Equation (13) to obtain

$$\begin{aligned} \mathbf{j}_g^w &= \omega_g^w \rho_g \mathbf{q}_g - \mathbf{D}_g^w \nabla \omega_g^w \\ &= - \left( \frac{\omega_g^w}{1 - \omega_g^w} + 1 \right) \mathbf{D}_g^w \nabla \omega_g^w = - \left( \frac{1}{1 - \omega_g^w} \right) \mathbf{D}_g^w \nabla \omega_g^w. \end{aligned} \quad (15)$$

In other words, the gas phase flux generated to balance the diffusion of air is able to induce a transport of vapour.

If an unsaturated soil closed to mass transfer is considered, air immobility only takes place at steady state regime. Therefore this assumption will not give exact results during the transient phases.

(b) Constant gas pressure assumption. In this case  $\mathbf{q}_g$  is neglected following the assumption that gas pressure gradient is zero then the total vapour flux is

$$\mathbf{j}_g^w = -\mathbf{D}_g^w \nabla \omega_g^w. \quad (16)$$

In this case no enhancement is obtained because no gas phase flow (considered as a whole) is taken into account. It is not necessary to calculate the air balance equation because gas pressure is assumed known.

### 3.4. GAS PRESSURE GRADIENT INDUCED BY VAPOUR MIGRATION IN A MASS CLOSED SYSTEM

If no assumption regarding gas phase mobility is considered, combination of (11) and (12) leads to

$$\mathbf{j}_g^w = \left( \frac{\omega_g^w}{1 - \omega_g^w} \right) \mathbf{j}_g^a - \left( \frac{1}{1 - \omega_g^w} \right) \mathbf{D}_g^w \nabla \omega_g^w. \quad (17)$$

Equation (17) reduces to (15) if  $\mathbf{j}_g^a = 0$  (case a) and, as mentioned above, this happens only at steady state conditions. During transient phases,  $\mathbf{j}_g^a$  is not zero in

general. The following result can be obtained from the condition of air immobility (dispersion is neglected and the soil is assumed isotropic)

$$\begin{aligned} \mathbf{j}_g^a &= \omega_g^a \rho_g \mathbf{q}_g - \mathbf{D}_g^a \nabla \omega_g^a = 0, \\ \rho_g \mathbf{q}_g &= \frac{1}{\omega_g^a} \mathbf{D}_g^a \nabla \omega_g^a = -\frac{1}{(1 - \omega_g^w)} \mathbf{D}_g^w \nabla \omega_g^w, \\ \nabla P_g &= \frac{\tau}{k} \frac{\mu_g \phi S_g D}{(1 - \omega_g^w) k_{rg}} \nabla \omega_g^w = \frac{\tau}{k} A \nabla \omega_g^w \quad (A > 0). \end{aligned} \quad (18)$$

This dependence of gas pressure gradient on vapour mass fraction gradient is an important point. From (18), it can be seen that a factor controlling the gas pressure gradient is the ratio between the material parameters tortuosity ( $\tau$ ) and intrinsic permeability ( $k$ ).

### 3.5. LIQUID PRESSURE GRADIENT INDUCED BY VAPOUR MIGRATION IN A MASS CLOSED SYSTEM

In a similar way as described in 3.4., liquid pressure gradient induced by vapour migration can be obtained as a function of vapour mass fraction. This is derived from the condition of mass of water conservation at steady state regime (dispersion is neglected and the soil is assumed isotropic)

$$\begin{aligned} \mathbf{j}_l^w + \mathbf{j}_g^w &= 0 = \rho_l \mathbf{q}_l - \left( \frac{1}{1 - \omega_g^w} \right) \mathbf{D}_g^w \nabla \omega_g^w, \\ \rho_l \mathbf{q}_l &= \left( \frac{1}{1 - \omega_g^w} \right) \mathbf{D}_g^w \nabla \omega_g^w, \\ \nabla P_l &= -\frac{\tau}{k} \frac{\mu_l \phi \rho_g S_g D}{\rho_l k_{rl} (1 - \omega_g^w)} \nabla \omega_g^w = -\frac{\tau}{k} B \nabla \omega_g^w \quad (B > 0), \end{aligned} \quad (19)$$

where the vapour flux ( $\mathbf{j}_g^w$ ) has been calculated from Equation (17) plus the condition of air immobility ( $\mathbf{j}_g^a = 0$  at steady state regime). It can be seen that liquid pressure gradient is proportional to the ratio between tortuosity ( $\tau$ ) and intrinsic permeability ( $k$ ) but it develops with opposite sign.

In Section (5) these relationships (Equations 18 and 19) will be used to obtain an important result for vapour migration in low permeability soils.

## 4. Intrinsic Permeability in Clays

### 4.1. MEASURED INTRINSIC PERMEABILITY IN CLAYS

A very low intrinsic permeability is encountered in clays when this parameter is measured under water saturated conditions. In contrast much higher values are observed when, under unsaturated or dry conditions, the permeability to gas is

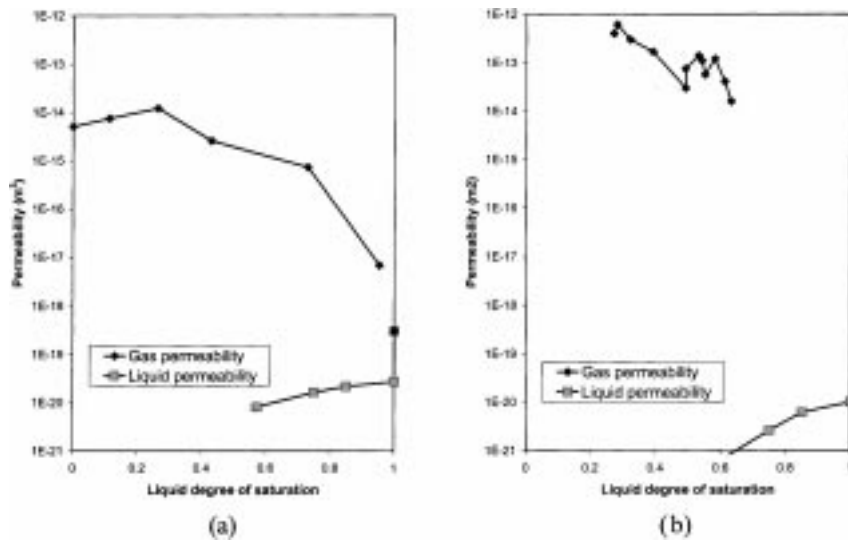


Figure 4. Compiled data on permeability (in  $m^2$ ) of clays to gas and water. (a) Boom Clay (Volkaert *et al.*, 1994), (b) Febex Clay (Villar, 1998).

measured. Figure 4 shows examples of measurements in Boom clay and Febex clay.

In the clays considered for these permeability determinations, the dry density ranged from  $1.65$  to  $1.7 \text{ g/cm}^3$ . Assuming that the variations of porosity are small (and this is difficult to be guaranteed because wetting induces very relevant swelling of these soils) it is clear that a single intrinsic permeability can not be used for these clays. If the value of intrinsic permeability for water was used, the gas permeability that one would obtain is several orders of magnitude smaller than the actual values. This is because in these plots the curves for gas permeability would be lowered until the value for  $S_l = 0$  of gas permeability would be the same as the value for  $S_l = 1$  of liquid permeability.

#### 4.2. A NEW MODEL FOR INTRINSIC PERMEABILITY OF CLAYS

A model that gives highly different mobilities to gas and water is necessary to model the permeability values that take place in expansive clays. A simple way to achieve this objective is to use a double porosity structure. Intrinsic permeability can be considered a function only of the macro porosity and macro porosity changes as water content changes. Figure 5 shows a schematic representation of the distribution of the macro and micro porosity's in the soil. It must be noticed that the total porosity is assumed constant in this work and that a single degree of saturation applies to macro, micro and total porosity. These assumptions permit a relatively simple approach to the problem because mechanical effects are neglected and a double porosity approach for balance equations is not required.

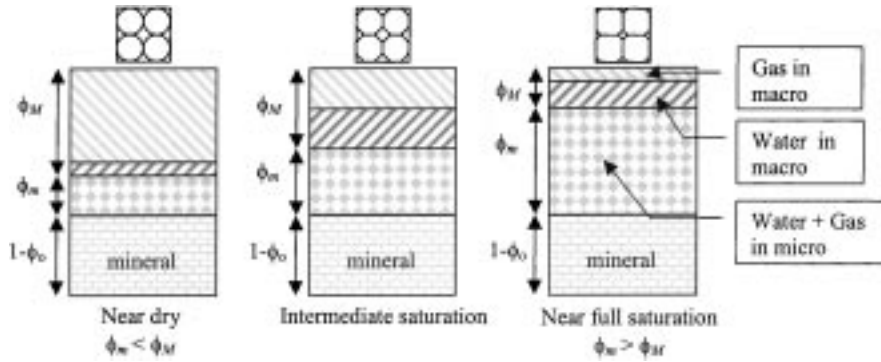


Figure 5. Schematic representation of the distribution of total porosity ( $\phi$ ), macro or flowing porosity ( $\phi_M$ ) and micro or no flowing porosity ( $\phi_m$ ). As water content increases, micro porosity increases while macro porosity decreases. Solid phase (mineral + micro porosity) increases its volume consuming macro porosity.

If  $M$  stands for macro and  $m$  for micro, the following relationships are proposed

$$\begin{aligned}\phi_o &= \phi_M + \phi_m, \\ \phi_M &= \phi_o \exp(-\beta S_1),\end{aligned}\quad (20)$$

where an exponential function has been introduced as a first approximation for the dependence on degree of saturation. It is assumed that when the medium is nearly dry, practically all porosity is macro porosity while when the medium tends to saturation, all porosity is micro porosity. Using this definition, intrinsic permeability will be calculated as

$$\mathbf{k} = \mathbf{k}(\phi_M) = \mathbf{k}(\phi_o - \exp(-\beta S_1)).\quad (21)$$

In Equation (21) any available function of intrinsic permeability on porosity can be used as a first approximation, for instance, Kozeny's relationship (Bear, 1972). Since permeability is a function of macro porosity only, water in micro porosity is assumed to be immobile.

The double porosity distribution proposed here is only used for calculation of intrinsic permeability. After retention curve is included in Equation (21), a relationship between intrinsic permeability and capillary pressure is obtained. This means that the variable  $\phi_M$  is only an intermediate physical concept to explain the proposed equations. The model will have to be improved in order to incorporate it in a general double porosity approach for thermo-hydro-mechanical analysis in unsaturated soils. In fact, the micro/macro porosity distribution would have to be consistent with the mechanical model. However, the double structure concept used here is conceptually consistent with the one used to explain the observed mechanical behaviour of such clay under stress and suction loading processes (Alonso and Gens, 1999; Alonso *et al.*, 1995).

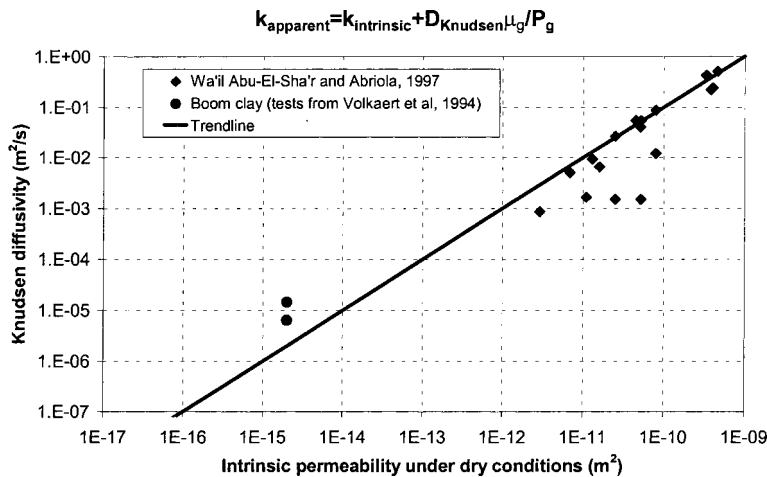


Figure 6. Knudsen diffusivity as a function of intrinsic permeability.

#### 4.3. OTHER ENHANCEMENT PHENOMENA OF GAS FLOW

Knudsen diffusion or Klinkenberg effect can also explain a higher permeability of the gas phase when pores are small. In Equation (8) a simple way to consider this process has been included. In order to see the relative influence of this process, that is, if it can explain that the permeability of the gas phase increases by orders of magnitude, values of  $D_k$  in Equation (8) are included in Figure 6. A number of experimental tests have been carried out by Wa'il Abu-El-Sha'r and Abriola (1997) on high permeability soils and the obtained Knudsen diffusivities (Figure 6) show a good correlation with intrinsic permeability. Here, Knudsen diffusivities for a much lower intrinsic permeability soil have been incorporated. These latter have been calculated from experimental results on tests described in Volkaert *et al.* (1994). Although the clayey soil that has been investigated by Volkaert *et al.* (1994) show a much lower intrinsic permeability to water, for gas the value is around  $10^{-15} \text{ m}^2$  (see Figure 4) which seems still a high value for this clay (Boom clay).

In any case, the relative increase of intrinsic permeability due to Knudsen diffusion is much less than an order of magnitude (of the order of 1.5–2 times for pressure between 0.125 and 0.3 MPa). Therefore, it can not be the cause that explains the higher mobility of gas phase. Of course, if the Knudsen diffusivity was calculated on the basis of the intrinsic permeability found under saturated conditions for this clay, the values encountered would have been much higher. This would also be inconsistent because the tendency in Figure 6 would be lost.

## 5. Modelling Drying Induced by Temperature Gradients

In this section, we want to show experimental evidence of the capabilities of the model proposed. For this purpose a heating test carried out at CIEMAT laboratories

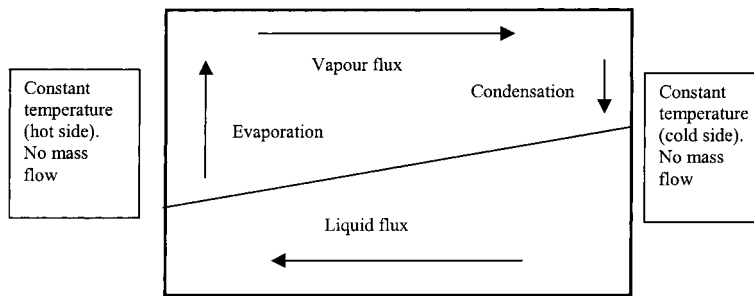


Figure 7. Schematic representation of fluxes of water induced by a temperature gradient in a one-dimensional domain.

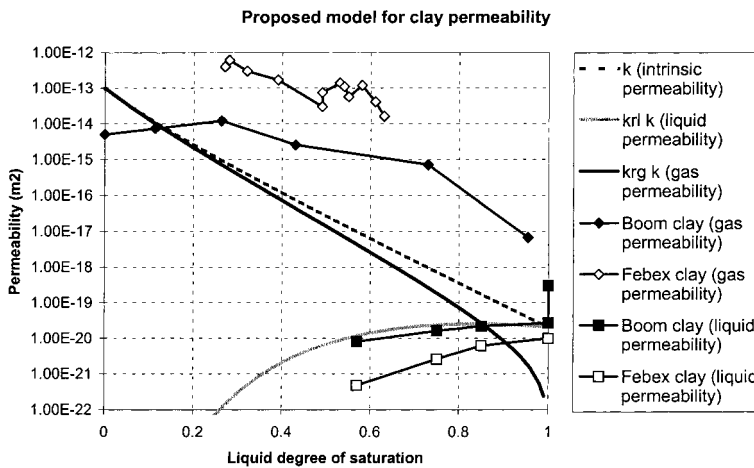


Figure 8. Curves of permeability to gas and liquid phases according to the proposed model. Experimental results for Boom clay and Febex clay are included for reference.

has been chosen (Villar *et al.*, 1997). In the test chosen here (CTF1) a temperature gradient ( $9^{\circ}\text{C}/\text{cm}$ ) is imposed on a sample composed by four layers of clay (2.5 cm each). There is no water flow through the boundaries and the initial dry density is  $1.65\text{ g}/\text{cm}^3$ . After 14 days, water content and dry density were measured in the four different layers. From these measurements, the experimental degree of saturation curve in the sample has been obtained (see Figure 9). Although a change of dry density from the initial value to  $1.48\text{--}1.60\text{ g}/\text{cm}^3$  (higher value near heater) the mechanical effects are ignored in this work. Figure 7 shows the water fluxes induced by the temperature gradient.

The simulation of the test has been performed using the variables and parameters that are presented in Table I. In Figure 8 the permeability for each phase (in  $\text{m}^2$ ) is plotted together with the intrinsic permeability curve. The parameters chosen lead to values which are in qualitative agreement with the experimental results shown (from Figure 4). The results of the simulation are shown in Figure 9. It can be seen that a quite good agreement with the measurements is obtained with this

Table I. Variables and parameters used for the simulation of the CIEMAT test CTF1

Description	Value	Comments
Sample length	10 cm	From test CTF1
Clay porosity ( $\phi_o$ )	0.44	Total porosity (macro and micro)
Initial gas pressure ( $P_g$ )	0.1 MPa	Atmospheric pressure
Initial liquid pressure ( $P_l$ )	-75.0 MPa	From retention curve
Initial temperature ( $T$ )	30°C	From test CTF1
Thermal conductivity	$\lambda = \lambda_{dry}^{S_g} \lambda_{sat}^{S_l}$ $\lambda_{dry} = 0.5 \text{ W/mk}$ $\lambda_{sat} = 1.28 \text{ W/mK}$	Adopted model (weighted geometric average) on the basis of experimental results obtained by Villar (1994).
Liquid phase relative permeability	$k_{rl} = S_l^{12}$	Estimated for the proposed permeability model*
Gas phase relative permeability	$k_{rg} = S_g$	Estimated for the proposed permeability model *
Vapour molecular diffusivity ( $D, \text{m}^2/\text{s}$ )	$5.9 \times 10^{-12} \frac{(T, ^\circ\text{C})^{2.3}}{(P_g, \text{MPa})}$	Philip and de Vries (1957) (Tortuosity, $\tau = 1$ ).
Retention curve parameters ( $P_o, \lambda$ )	18 MPa, 0.38	Adopted model (van Genuchten) on the basis of experimental results obtained by Villar (1994).
Boundary temperatures ( $T_1, T_2$ )	120, 30 °C	From test CTF1
Macro/micro porosity distribution.	$\phi_M = \phi_o \exp(-\beta S_l)$ $\phi_m = \phi_o - \phi_M$ $\phi_o = 0.44, \quad \beta = 4.75$	Adopted macro/micro porosity distribution for the proposed permeability model.*
Intrinsic permeability	$\mathbf{k}(\phi_M) = \mathbf{I} k_o \frac{(1-\phi_o)^2}{\phi_o^3} \frac{\phi_M^3}{(1-\phi_M)^2}$ $\phi_o = 0.44, \quad k_o = 10^{-13} \text{ M}^2$	Kozeny's intrinsic permeability function. Used with Macro porosity instead of total porosity.*

\*Relationships and parameters in this work to model CTF1 test.

analysis, except for the dry zone. It is important to mention that the high mobility of the gas phase is a crucial point for the drying to occur. In fact, if the intrinsic permeability of the medium were considered constant (of the order of  $10^{-19} \text{ m}^2$ ) vapour diffusion would have induced a high gas pressure gradient (according to Equation 18). In such case, the steady state regime obtained would not have shown this profile of degree of saturation but a nearly constant value indicating that the drying is prevented.

In order to understand better the effect of permeability on drying, a relationship will be derived from Equations (18) and (19). These equations have been intro-



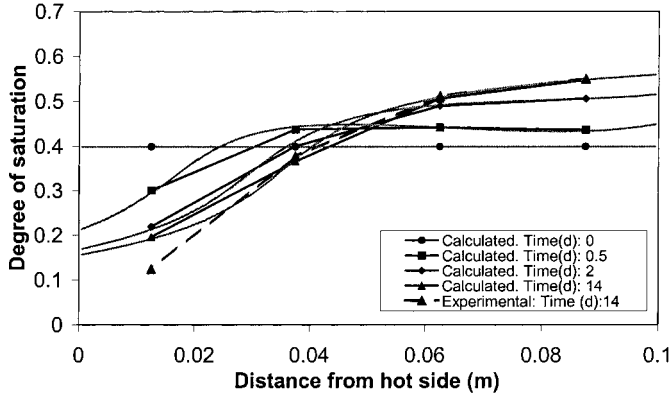


Figure 9. Interpretation of a lab-heating test performed in CIEMAT. Profiles of degree of saturation for different times during the calculation and experimental results for 14 days. Averaged values are shown with symbols while the full profile is shown in grey.

duced in the gradient of mass fraction split in terms of the state variables considered here ( $P_g$ ,  $P_l$  and  $T$ ), that is,

$$\begin{aligned}\nabla\omega_g^w &= \frac{\partial\omega_g^w}{\partial P_g}\nabla P_g + \frac{\partial\omega_g^w}{\partial P_l}\nabla P_l + \frac{\partial\omega_g^w}{\partial T}\nabla T, \\ \nabla\omega_g^w &= \frac{\partial\omega_g^w}{\partial P_g}\frac{\tau}{k}A\nabla\omega_g^w - \frac{\partial\omega_g^w}{\partial P_l}\frac{\tau}{k}B\nabla\omega_g^w + \frac{\partial\omega_g^w}{\partial T}\nabla T, \\ \nabla\omega_g^w &= \frac{(\partial\omega_g^w/\partial T)\nabla T}{[1 - (\tau/k)(\partial\omega_g^w/\partial P_g)A + (\tau/k)(\partial\omega_g^w/\partial P_l)B]} = C\frac{\partial\omega_g^w}{\partial T}\nabla T, \quad (22)\end{aligned}$$

where  $A (> 0)$  and  $B (> 0)$  have been defined in Equations (18) and (19), respectively, and  $C$  is defined here. Using the ideal gases law, mass fraction of vapour can be written as

$$\omega_g^w = \frac{P_v M_v}{P_v M_v + P_a M_a} = \frac{P_v M_v}{P_v M_v + (P_g - P_v) M_a}, \quad (23)$$

where  $P_v$  is the vapour pressure and  $P_a$  the air pressure. If psychrometric effects are neglected ( $\partial\omega/\partial P_l = 0$ ) and (23) is used, it follows that  $\partial\omega/\partial P_g < 0$  ( $C$  is positive). Equation (22) indicates that for high permeability soils vapour concentration gradient is proportional to temperature gradient only ( $C \approx 1$ ). In contrast, for low permeability soils (as happens with expansive clays) vapour concentration gradient is proportional to permeability, among other variables ( $C \propto k$ ).

Therefore the lowest the intrinsic permeability, the lowest the vapour mass fraction gradient and the lowest the drying induced by a temperature gradient.

In order to show the influence of this effect on drying a sensitivity analysis to the parameters  $k_o$  and  $\beta$  has been performed for the modelling of the experiment of heating. Table II shows the values adopted and Figure 10 the profiles of degree

Table II. Parameter values for sensitivity calculations

$k_o(m^2)$	$\beta$	$k_{(gas)}(m^2)$	$k_{(liquid)}(m^2)$	Case
$10^{-13}$	4.75	$10^{-13}$	$2.11 \times 10^{-20}$	0
$10^{-15}$	3.2	$10^{-15}$	$2.17 \times 10^{-20}$	1
$10^{-18}$	1.0	$10^{-18}$	$2.05 \times 10^{-20}$	2

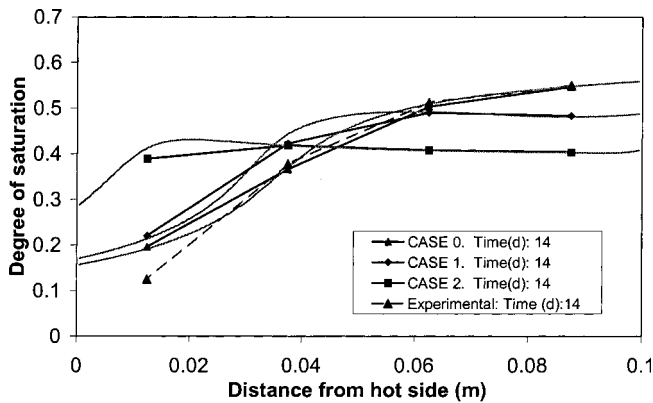


Figure 10. Sensitivity to intrinsic permeability function. Profiles for degree of saturation at 14 days for different functions of permeability. Averaged values are shown with symbols while the full profile is shown in grey.

of saturation at 14 days for each case. It is clearly shown that gas mobility plays an important role. In the three cases compared in Figure 9 the intrinsic permeability to liquid phase is the same but the intrinsic permeability to the gas phase has been reduced. It can be seen that as gas mobility decreases the drying effects also reduce.

## 6. Conclusions

The main objective of this paper was to contribute to the understanding of water evaporation and vapour transport in the context of unsaturated soils. Several research works related to radioactive waste disposal in geological media have motivated this work. In fact, the maximum temperatures permitted are in some cases above  $100^{\circ}\text{C}$ , but even in the case that temperature was limited to  $100^{\circ}\text{C}$  there is a need to treat in an appropriate way the gas phase.

Firstly, we have discussed the two main existing approaches for modelling thermal effects in unsaturated porous soils and the main differences have been highlighted. It has been shown that when the NUS (nonisothermal unsaturated soil) approach is used to model an initially saturated soil that develops small capillary pressures, phase change tends to behave in the same way, as one would obtain with

the GR (geothermal reservoir) approach. In this case the phase change diagram of water controls desaturation.

Secondly, transport processes have been discussed. The relative importance of terms that appear in a general formulation has been explained. Also, the question of vapour flux enhancement has been treated when the cause is related to air immobility. Particularly the problem of mass transfer induced by temperature gradients has been treated. Gas and liquid pressure gradients are developed by a thermal gradient in an unsaturated soil due to water evaporation–migration–condensation.

Finally, a model for intrinsic permeability for clays that change its structure when wetting–drying occurs is presented. This model is necessary for modelling the moisture content profiles induced by temperature gradients in low permeability soils. The proposed model explains at the same time the higher gas mobility encountered in clays compared to the water mobility and the process of drying induced by temperature gradients. In order to show the capabilities of the model and formulation, an experimental test has been modelled and the calculated results show a very good agreement with the measurements. Also some sensitivity calculations have been carried out to demonstrate the necessity of the dependence of intrinsic permeability on liquid water content introduced.

### Appendix 1. Sensitivity to Phase Change Under Different Capillary Effects

Using the retention curve given in Section 2 (Equation 3), different values of  $P_0$  have been chosen ( $1, 10^{-3}, 10^{-6}, 10^{-7}$  MPa) to study the sensitivity of phase change to different soil types. Since liquid and gas pressure will not be equal only one can be prescribed (when capillary pressure is neglected, constant vapour pressure implies constant water pressure and vice versa). If liquid pressure is prescribed, then vapour pressure will change. For the calculations performed here liquid pressure is assumed constant and equal to 0.1 MPa and the soil is considered saturated before heating. This means that air is not present in the soil. A sufficiently small amount can be considered initially dissolved in water as an artefact.

The following approximate relationships are used for surface tension of water–gas (Pruess, 1987):

$$\begin{aligned}\sigma(T) &= (1 - 0.625a)(0.2358a^{1.256}) \quad a = \frac{374.15 - T}{647.3} \quad T < 360^\circ\text{C} \\ \sigma(T) &= 0.0019106\exp(0.05(360 - T)) \quad T > 360^\circ\text{C}\end{aligned}\quad (\text{A1.1})$$

and for vapour density (ideal gas + phase diagram + psychrometric law)

$$\begin{aligned}\rho_v &= \frac{P_v M_w}{R(273 + T)}, \\ P_v(T, P_g - P_l) &= 136075\exp\left(\frac{-5239.7}{273 + T}\right)\exp\left(\frac{-(P_g - P_l)M_w}{R(273 + T)\rho_l}\right).\end{aligned}\quad (\text{A1.2})$$

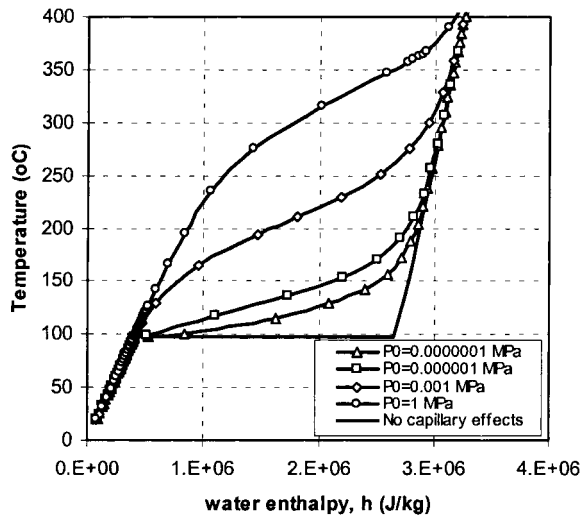


Figure A1.1. Temperature vs water enthalpy for heating soils with different retention curves.

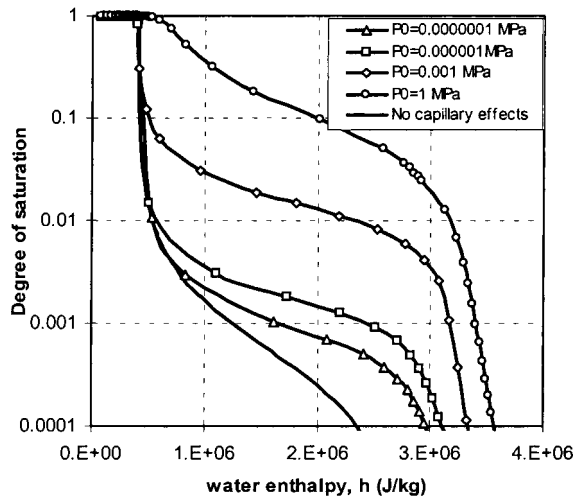


Figure A1.2. Degree of saturation vs water enthalpy for heating soils with different retention curves.

Figure A1.1 shows the temperature variation as a function of the enthalpy. It can be seen that temperature does not remain constant after 100°C but it increases with a slope, which in fact is lower as capillary effects decrease (lower  $P_0$ ). In order to understand better this temperature variation, the diagram of degree of saturation is shown in Figure A1.2. Due to capillary effects, for a given water enthalpy, an amount of water has not evaporated (degree of saturation is higher than the corresponding value for the phase diagram of water). Consequently, heat is used to increase temperature instead of being used to evaporate the amount of

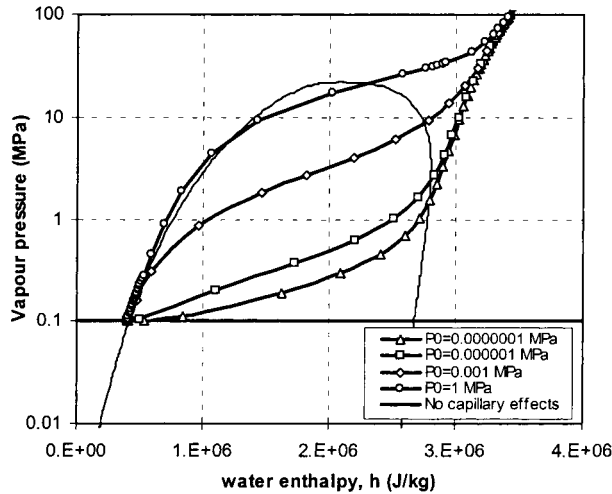


Figure A1.3. Vapour pressure vs water enthalpy for heating soils with different retention curves.

water that cannot evaporate. The curves show a tendency towards the curve for zero capillary pressure as capillary effects reduce (i.e. for lower values of  $P_0$ ).

Figure A1.3 shows the variation of vapour pressure as a function of water enthalpy. In this plot, the curves that define the regions in the phase diagram for water (Figure 1) are also included. Since temperature increases after 100°C and liquid pressure is maintained at 0.1 MPa, vapour pressure increases in accordance with the phase diagram for water.

From Figures A1.1 to A1.3, it can be concluded that the NUS approach tends to the GR approach when capillary effects decrease if the soil does not contain air. It should be mentioned, however, that the NUS approach still calculates degree of saturation as a function of capillary pressure, therefore it may become less robust than the GR approach when this dependence is lost. When temperatures are high, the NUS approach for a soil without air tends also to the GR approach because the capillary effects decrease when surface tension decreases.

## Appendix 2. Balance Equations

### A2.1. MASS BALANCE OF WATER

Water is present in liquid and gas phases. The total mass balance of water is expressed as

$$\frac{\partial}{\partial t} (\omega_1^w \rho_1 S_l \phi + \omega_g^w \rho_g S_g \phi) + \nabla \cdot (\mathbf{j}_1^w + \mathbf{j}_g^w) = f^w, \quad (\text{A2.1})$$

where  $f^w$  is an external supply of water,  $\phi$  is porosity,  $\omega_\alpha^i$  is the mass fraction of species  $i$  in phase  $\alpha$ ,  $\rho_\alpha$  is the density of phase  $\alpha$ , and  $S_\alpha$  is the degree of saturation of phase  $\alpha$ .

### A2.2. MASS BALANCE OF AIR

Air is present in liquid and gas phases. The total mass balance of air is expressed as

$$\frac{\partial}{\partial t}(\omega_1^a \rho_1 S_1 \phi + \omega_g^a \rho_g S_g \phi) + \nabla \cdot (\mathbf{j}_1^a + \mathbf{j}_g^a) = f^a. \quad (\text{A2.2})$$

### A2.3. INTERNAL ENERGY BALANCE FOR THE MEDIUM

The equation for internal energy balance for the porous medium is established taking into account the internal energy in each phase ( $E_s$ ,  $E_l$ ,  $E_g$ )

$$\begin{aligned} \frac{\partial}{\partial t}(E_s \rho_s (1 - \phi) + E_l \rho_l S_l \phi + E_g \rho_g S_g \phi) + \\ + \nabla \cdot (\mathbf{i}_c + \mathbf{j}_{Es} + \mathbf{j}_{El} + \mathbf{j}_{Eg}) = f^Q, \end{aligned} \quad (\text{A2.3})$$

where  $\mathbf{i}_c$  is energy flux due to conduction through the porous medium, the other fluxes ( $\mathbf{j}_{Es}$ ,  $\mathbf{j}_{El}$ ,  $\mathbf{j}_{Eg}$ ) are advective fluxes of energy caused by mass motions and  $f^Q$  is an internal/external energy supply.

### Acknowledgements

The support of ENRESA and ANDRA through research grants is gratefully acknowledged.

### References

- Alonso, E. E., Lloret, A., Gens, A. and Yang, D. Q.: 1995, Experimental behaviour of highly expansive double structure clay, In: *Proc. 1st Int. Conf. On Unsaturated Soils*, Paris, Vol. 1, pp. 11–16.
- Alonso, E. E. and Gens, A.: 1999, Modelling Expansive Geomaterials, In: R. C. Picu and E. Kreml (eds), *4th Int. Conf. on Constitutive Laws for Engineering Materials*, Troy (New York).
- Bear J.: 1972: *Dynamics of Fluids in Porous Media*, American Elsevier Publishing Company.
- Bear, J. and Bachmat, Y.: 1986, Macroscopic modelling of transport phenomena in porous media. 2. Applications to mass, momentum and energy transport, *Transport in Porous Media* **1**, 241–269.
- Bear, J. and Gilman, A.: 1995, Migration of salts in the unsaturated zone caused by heating, *Transport in Porous Media* **19**, 139–156.
- Bird, R. B., Stewart, W. E. and Lightfoot, E. N.: (1960): *Transport Phenomena*, John Wiley, New York, 1960.
- Edlefson, N. E. and Anderson, A. B. C.: 1943, Thermodynamics of soil moisture, *Hilgardia* **15**(2), 31–298.
- Falta, R. W., Pruess, K., Javandel, I. and Witherspoon, P. A.: 1992, Numerical modelling of steam injection for the removal of nonaqueous phase liquids from the subsurface. 1. Numerical formulation, *Water Resour. Res.* **28**(2), 433–449.
- Faust, C. R. and Mercer, J. W.: 1979, Geothermal reservoir simulation: 1. Mathematical models for liquid- and vapour- dominated hydrothermal systems, *Water Resour. Res.* **15**(1), 23–30.

- Gens, A., Garcia-Molina, A. J., Olivella, S., Alonso, E. E., Huertas, F.: 1998, Analysis of full scale *in-situ* heating test simulating repository conditions, *Int. J. Num. Anal. Meth. Geomech.* **22**, 515–548.
- Milly, P. C. D.: 1982, Moisture and heat transport in hysteretic, inhomogeneous porous media: a matric head-based formulation and a numerical model, *Water Resour. Res.* **18**(3), 489–498.
- Olivella, S., Carrera, J., Gens, A., Alonso, E. E.: 1994, Non-isothermal multiphase flow of brine and gas through saline media, *Transport in Porous Media* **15**, 271–293.
- Olivella, S., Carrera, J., Gens, A., Alonso, E. E.: 1996a, Porosity variations in saline media caused by temperature gradients coupled to multiphase flow and dissolution/precipitation, *Transport in Porous Media* **25**, 1–25.
- Olivella, S., Gens, A., Carrera, J., Alonso, E. E.: 1996b, Numerical formulation for a simulator (CODE\_BRIGHT) for the coupled analysis of saline media, *Engng Comput.* **13**(7), 87–112.
- Philip, J. R. and de Vries, D. A.: 1957, Moisture movement in porous materials under temperature gradients, *EOS Trans. AGU* **38**(2), 222–232.
- Pollock, D. W.: 1986, Simulation of fluid flow and energy transport processes associated with high-level radioactive waste disposal in unsaturated alluvium, *Water Resour. Res.* **22**(5), 765–775.
- Pruess, K.: 1987, *TOUGH User's Guide*, Lawrence Berkeley Laboratory.
- Roberts, P. J., Lewis, R. W., Carradori, G. and Peano, A.: 1987, An extension of the thermodynamic domain of a geothermal reservoir simulator, *Transport in Porous Media* **2**, 397–420.
- van Genuchten, R.: 1980, A closed-form equation for predicting the hydraulic conductivity of unsaturated soils, *Soil Sci. Soc. Am. J.*, 892–898.
- Villar, M. V.: 1994, Modelling and validation of the thermo-hydraulic-mechanical and geochemical behaviour of the clay barrier, Final report 1991–1994, CIEMAT, Madrid.
- Villar, M. V., Fernandez, A. M. and Cuevas, J.: 1997, Full scale engineered barriers experiment in crystalline host rock, Caracterización Geoquímica de bentonita compactada: efectos producidos por flujo termohidráulico, Informe 70-IMA-M-0-2, Ciemat, Enresa.
- Villar, M. V.: 1998, Ensayos para el proyecto FEBEX, CIEMAT-report 70-IMA-L-5-51, prepared for ENRESA.
- Volckaert, G., Ortiz, L., De Cannière, P., Put, M., Horseman, S. T., Harrington, J. F., Fioravante, V. and Impey, M.: 1994, Modelling and experiments on gas migration in repository host rocks, MEGAS Project, Final Report, Phase 1.
- Wa'il Abu-El-Sha'r and Abriola, L. M.: 1997, Experimental assessment of gas transport mechanisms in natural porous media. Parameter estimation, *Water Resour. Res.* **33**(4), 505–516.